Charge regulation in ionic solutions: Thermal fluctuations and Kirkwood-Schumaker interactions

Nataša Adžić[1,*] and Rudolf Podgornik[1,2]

[1]*Department of Theoretical Physics, J. Stefan Institute, 1000 Ljubljana, Slovenia*

[2]*Department of Physics, Faculty of Mathematics and Physics, University of Ljubljana, 1000 Ljubljana, Slovenia*

(Received 21 December 2014; published 24 February 2015)

We study the behavior of two macroions with dissociable charge groups, regulated by local variables such as *p*H and electrostatic potential, immersed in a monovalent salt solution, considering cases where the net charge can either change sign or remain of the same sign depending on these local parameters. The charge regulation in both cases is described by the proper free-energy function for each of the macroions, while the coupling between the charges is evaluated on the approximate Debye-Hückel level. The charge correlation functions and the ensuing charge fluctuation forces are calculated analytically and numerically. Strong attraction between like-charged macroions is found close to the point of zero charge, specifically due to asymmetric, anticorrelated charge fluctuations of the macroion charges. The general theory is then implemented for a system of two proteinlike macroions, generalizing the form and magnitude of the Kirkwood-Schumaker interaction.

DOI: 10.1103/PhysRevE.91.022715 PACS number(s): 87.15.km, 78.30.cd

I. INTRODUCTION

From the point of view of electrostatic interactions, proteins, such as ampholytes, are challenging objects since they carry a nonconstant charge, dependent on dissociation of chargeable molecular moieties such as N and C terminals as well as the (de)protonation of amino acid side groups [1–3]. Consequently, their behavior cannot be analyzed with the assumption of a constant charge [4], otherwise applicable for many (bio)colloidal systems [5], since it misses the crucial contribution of charge regulation and charge fluctuations to the interactions between macroions [6]. In fact, it has been known for some time that extremely-long-ranged attractive interactions occur between proteins in an aqueous solution with dissociable charge groups (amino acids) on the surface, close to their point of zero charge (PZC), as first elucidated by Kirkwood and Shumaker [7,8]. The Kirkwood-Shumaker (KS) derivation is based on the thermodynamic perturbation theory around a noninteracting state that takes into account protein charge fluctuations. In the case of no ionic screening, apart from the usual Coulomb interaction, they also obtain a fluctuation interaction that scales as an inverse second power of the separation between the macroions. This scaling form is fundamentally different from the van der Waals interactions, exhibiting an inverse sixth power [9], that stem from dipolar fluctuations and act between electroneutral bodies. In fact, it can be shown that it is a consequence of the monopolar charge fluctuations and does not exist for macroions with a strictly fixed charge distribution. Kirkwood-Shumaker interaction pertains only to systems with flexible charge equilibrium that possess a nonzero capacitance, where the net charge is not a constant but depends on the underlying dissociation processes [10], implying furthermore that the effective charge on the macroion, e.g. the protein surface, is regulated and responds to the local solution conditions: *p*H, electrostatic potential, salt concentration, spatial dielectric constant profile, and the presence of other vicinal charged groups [11]. While the effects of charge regulation were analyzed on various levels in the mean-field approximation [10,12–18], the fluctuation effects have not received a proportional amount of attention.

Recently, the KS theory experienced renewed interest when it was shown, using detailed Monte Carlo simulations [19], that indeed there exists an interaction between proteins that has the same salient features as the original approximate form of the KS interaction. An important step further was achieved by consistently including the charge-regulation free energy [10], derivable from the Parsegian-Ninham model [20], in the theoretical framework that allowed one to derive analytically and exactly the interaction free energy on the Gaussian fluctuation level [21], leading to an exact form of the KS interaction for the three-dimensional system with planar geometry. The full exact solutions for charge-regulation interaction, beyond the Gaussian fluctuation ansatz, have been found also in the case of a family of one-dimensional models solvable by the transfer-matrix formalism [22].

The aim of this paper is to present an improved theory of fluctuation interaction for two small and distant spherical macroions subject to charge regulation. The problem is formulated in a way that allows for decoupling of the charge-regulation part and the interaction part, of which the former can be treated exactly while the latter can be dealt with on the Debye-Hückel (DH) level. This allows us to derive a closed-form expression for the total interaction and compare it with various approximate forms, including the original KS expression. We show that our generalized fluctuation interaction reduces exactly to the KS result in the limit of large separations between macroioins, where the macroion charge autocorrelation function is assumed to be independent of the separation between them, consistent with the original KS perturbation theory derivation. This assumption, implicit in the original KS derivation, breaks down for any finite separation. Apart from going beyond this limitation of the original theory of KS interactions, we are also able to go beyond the KS result in terms of deriving realistic *p*H and ionic-strength-dependent interactions between protein macroions with known amino acid composition.

The paper is arranged as follows. In Sec. II we introduce a model consisting of two spherical macroions immersed in a monovalent salt solution, with charge-regulated surface

*natasa.adzic@ijs.si

charges described with an appropriate free-energy term. The theory of electrostatic interactions for such a system is derived using the field-theoretic approach, described in Appendix A. Three different cases of charge regulation are considered (Sec. III): a fully symmetric system, consisting of two identical macroions with both charges spanning the interval $[-e,e]$; a semisymmetric system, composed of two identical macroions with charges spanning the asymmetric interval $[-e,(\alpha-1)e]$ ($\alpha>1$); and a completely asymmetric system composed of one negative and one positive macroion with charges $[-e,0]$ and $[0,e]$, respectively. For all three cases we calculate the average charge, the charge-charge cross-correlation function, the charge-charge autocorrelation function, and the total interaction potential obtained numerically using the exact evaluation of the full partition function as well as via two simplifying and illuminating approximation methods (Sec. IV): the saddle-point method and the Gaussian approximation method, both giving an analytical closed form for the full charge-regulation interaction, including the thermal fluctuations. In Sec. V we show how this theory can be generalized to be applicable to a system of proteinlike macroions with specific amino acid composition. In Sec. VI we present a summary and comment on the connection with experiments and simulations.

II. MODEL

We consider a model system composed of two charged spherical macroions in a 1:1 salt solution (Fig. 1). The charge of the macroions is not constant, but is described by a dissociation surface free-energy density cost corresponding to the Parsegian-Ninham charge-regulation model, as discussed in [21], of the general lattice-gas form

$$f_0(\varphi(\vec{r})) = i\sigma_0\varphi(\vec{r}) - \alpha k_B T \frac{\sigma_0}{e_0}\ln\left(1+be^{i\beta e_0\varphi(\vec{r})}\right), \quad (1)$$

where e_0 is the elementary charge, β is the inverse of the thermal energy k_BT. α quantifies the number of dissociation sites, and $\ln b = \beta\mu_S$, where μ_S is the free energy of charge

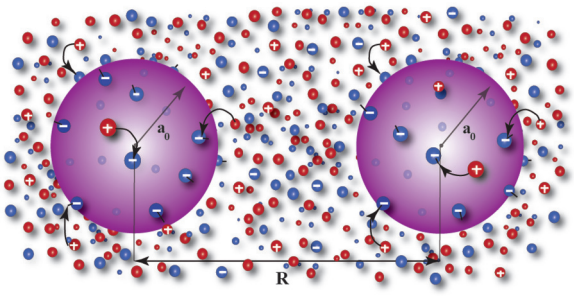

FIG. 1. (Color online) Schematic representation of the model: two charge-regulated macroions immersed in a 1:1 salt solution, with positive and negative ions indicated in red and blue, respectively. The dissociation sites and the dissociation process itself at the surface of the macroions are indicated with arrows. The solution is composed of salt ions that can be exchanged with the surface sites. In the Ninham-Parsegian model of charge regulation, the charge group dissociation proceeds through (de)protonation of the dissociable charge groups. In the case of proteins these are the dissociable amino acids.

dissociation. In the case of protonation of the surface charge one furthermore has $\ln b = -\ln 10(p\mathrm{H}-p\mathrm{K})$ [21], where pK is the dissociation constant and pH indicates its value in the bulk, differing from the local value of pH at the dissociation sites exactly by the value of the local electrostatic potential, as implied by the second term in the logarithmic function of the above equation. The local electrostatic potential also depends on the ionic strength of the solution as well as on the vicinity of other dissociable charge groups or macroions [16].

Above $\varphi(\vec{r})$ is the local fluctuating potential that needs to be integrated over to get the final partition function. The mean-field Poisson-Boltzmann (PB) approximation is obtained by identifying $\varphi(\vec{r})\to i\phi = i\phi_{\mathrm{PB}}$ [21]. The total dissociation free energy for a spherical macroion of radius a_0, sufficiently small so that one can assume that the electrostatic potential is uniform over its surface $\varphi(|\vec{r}|=a_0)=\varphi$, can be written in the form

$$\begin{aligned} f(\varphi) &= \oint_S f_0(\varphi(\vec{r}))d^2\vec{r} \\ &\to iNe_0\varphi - \alpha k_BTN\ln\left(1+be^{i\beta e_0\varphi}\right), \end{aligned} \quad (2)$$

where N is the number of absorption sites satisfying $\int dS\,\sigma_0 = Ne_0$ and $\alpha>1$ is a coefficient of asymmetry determining the width of the interval spanned by the particle's effective charge $e(\phi)$ as a function of the mean-field potential on its surface $\phi=\phi(a_0)$:

$$\begin{aligned} e(\phi=\phi(a_0)) &= \frac{\partial f(\phi)}{\partial\phi} \\ &= e_0N\left[\frac{\alpha}{2}-1-\frac{\alpha}{2}\tanh\left(-\frac{1}{2}(\ln b-\beta e_0\phi)\right)\right]. \end{aligned} \quad (3)$$

The effective charge of the macroion can thus fluctuate in the interval $-Ne_0<e<(\alpha-1)Ne_0$, $\alpha>1$. When $\alpha=2$ the charge interval is by definition symmetric $[-Ne_0,Ne_0]$. All of the expressions for the charge regulation referred to above are just variants of the surface lattice-gas free energies [21] with a variable number of dissociation sites that describe the dissociation of the charge moieties on the surface of the macroions. In addition we have taken the limit of small macroions, implying that the surface potential on the macroions is a constant $f(\varphi)=\oint_{|\vec{r}|=a_0} f_0(\varphi(\vec{r}))d^2\vec{r}$.

Assuming that the fluctuating electrostatic potential of one macroion is $\phi_1(a)=\varphi_1$ and of the other one is $\phi_2(a)=\varphi_2$, located at $\vec{r}_1$ and $\vec{r}_2$, respectively, the partition function of the system can be derived in the field-theoretic form (see Appendix A)

$$\mathcal{Z} = \int\int d\varphi_1 e^{-\beta f(\varphi_1)}G(\varphi_1,\varphi_2)e^{-\beta f(\varphi_2)}d\varphi_2, \quad (4)$$

where the partition function has already been normalized by dividing by the bulk system partition function [23], obtained for $f(\varphi)=0$, and $G(\varphi_1,\varphi_2)$ is the propagator of the field, defined with the values of the potential φ_1 and φ_2 at the location of the first and the second particle, respectively, derived in

Appendix A:

$$G(\varphi_1,\varphi_2)=\exp\left[-\frac{\beta}{2}\begin{pmatrix}\varphi_1\\ \varphi_2\end{pmatrix}^T\begin{pmatrix}G(\vec{r}_1,\vec{r}_1) & G(\vec{r}_1,\vec{r}_2)\\ G(\vec{r}_1,\vec{r}_2) & G(\vec{r}_2,\vec{r}_2)\end{pmatrix}^{-1}\begin{pmatrix}\varphi_1\\ \varphi_2\end{pmatrix}\right], \tag{5}$$

where the matrix of the Green's functions for the bulk composed of a 1:1 electrolyte in the DH approximation is given as

$$\begin{pmatrix}G(\vec{r}_1,\vec{r}_1) & G(\vec{r}_1,\vec{r}_2)\\ G(\vec{r}_1,\vec{r}_2) & G(\vec{r}_2,\vec{r}_2)\end{pmatrix}=\begin{pmatrix}\frac{1}{4\pi\epsilon\epsilon_0}\frac{e^{-\kappa a}}{a} & \frac{1}{4\pi\epsilon\epsilon_0}\frac{e^{-\kappa R}}{R}\\ \frac{1}{4\pi\epsilon\epsilon_0}\frac{e^{-\kappa R}}{R} & \frac{1}{4\pi\epsilon\epsilon_0}\frac{e^{-\kappa a}}{a}\end{pmatrix}. \tag{6}$$

Here we assume that the two macroions cannot come closer than $a = 2a_0$. Variations on the above form are possible and would contain the factor $\frac{e^{-\kappa(R-a)}}{R(1+\kappa a)}$ for the separation dependence of $G(\vec{r},\vec{r}\,)$. We will comment on the detailed choice of the form for the DH interaction later.

The charge-regulation energy term $e^{-\beta f(\varphi)}$ can now be expanded as a binomial [22]

$$\begin{aligned}e^{-\beta f(\varphi)} &= e^{-i\beta N e_0\varphi}(1+be^{i\beta e_0\varphi})^{\alpha N}\\ &= \sum_{n=0}^{\alpha N}\binom{\alpha N}{n}b^n e^{-i\beta N e_0\varphi}e^{i\beta e_0 n\varphi}.\end{aligned} \tag{7}$$

The integral (4) then becomes

$$\begin{aligned}\mathcal{Z} = \frac{1}{\mathcal{Z}_0}\int\int d\varphi_1 d\varphi_2 \sum_{n}^{\alpha N}\sum_{n'}^{\alpha N} a_n a_{n'} e^{-i\beta e_0(N-n)\varphi_1}\\ \times\exp\left[-\frac{\beta}{2}\begin{pmatrix}\varphi_1\\ \varphi_2\end{pmatrix}^T\begin{pmatrix}G(\vec{r}_1,\vec{r}_1) & G(\vec{r}_1,\vec{r}_2)\\ G(\vec{r}_1,\vec{r}_2) & G(\vec{r}_2,\vec{r}_2)\end{pmatrix}^{-1}\begin{pmatrix}\varphi_1\\ \varphi_2\end{pmatrix}\right.\\ \left.\times e^{-i\beta e_0(N-n')\varphi_2}\right],\end{aligned} \tag{8}$$

where $a_n(\alpha) = \binom{\alpha N}{n} b^n$ for any α.

Introducing the dimensionless variables $\tilde{R} = \kappa R$ and $\tilde{a} = \kappa a$, one can rewrite the partition function for two equal macroions with both charges allowed to vary in the interval $[-Ne_0, Ne_0]$ in the form

$$\mathcal{Z} = \sum_{n}^{2N}\sum_{n'}^{2N} a_n(2)a_{n'}(2)e^{-\beta\mathcal{F}_{N,N}(n,n',\tilde{R})}, \tag{9}$$

where we introduced $\mathcal{F}_{N,N}(n,n',\tilde{R})$ as

$$\begin{aligned}\mathcal{F}_{N,N}(n,n',\tilde{R}) = \frac{e_0^2\kappa}{8\pi\epsilon\epsilon_0}\left(\frac{e^{-\tilde{a}}}{\tilde{a}}[(N-n)^2+(N-n')^2]\right.\\ \left.+2\frac{e^{-\tilde{R}}}{\tilde{R}}(N-n)(N-n')\right).\end{aligned} \tag{10}$$

Clearly, we have incorporated exactly the charge-regulation free energy for each of the macroions, while the electrostatic coupling between the two macroions is included approximately via the DH propagator. The configuration of this particular example is symmetric, as the two macroions are identical and are described by the same charge-regulation free energy. The asymmetric configuration, corresponding to unequal charge-regulation free energies for the two macroions, is addressed next.

In order to describe two equal macroions with a regulated charge in the interval $-Ne_0 < e < 0$ we take as a model expression (2) with $\alpha = 1$, i.e.,

$$f(\varphi) = iMe_0\varphi - \alpha k_B T N\ln(1+be^{i\beta e_0\varphi}), \tag{11}$$

where $M = N$, and with the partition function

$$\mathcal{Z} = \sum_{n}^{N}\sum_{n'}^{N} a_n(1)a_{n'}(1)e^{-\beta\mathcal{F}_{N,N}(n,n',\tilde{R})}. \tag{12}$$

Furthermore, charge regulation in the interval $0 < e < Ne_0$ is described by

$$f(\varphi) = -k_B T N\ln(1+be^{i\beta e_0\varphi}), \tag{13}$$

corresponding to the protonization of neutral state ($M = 0$), with the partition function for two equal macroions obtained in the form

$$\mathcal{Z} = \sum_{n=0}^{N}\sum_{n'=0}^{N} a_n(1)a_{n'}(1)e^{-\mathcal{F}_{0,0}(n,n',\tilde{R})}. \tag{14}$$

Finally, for an asymmetric case where the two macroioins are different, one with charge in the allowed interval $[0, Ne_0]$ and the other one spanning the interval $[-Ne_0, 0]$, the partition function is obviously obtained in the form

$$\mathcal{Z} = \sum_{n=0}^{N}\sum_{n'=0}^{N} a_n(1)a_{n'}(1)e^{-\mathcal{F}_{N,0}(n,n',\tilde{R})}. \tag{15}$$

These results for the partition function derived above can be written succinctly in a single formula as

$$\mathcal{Z} = \sum_{n}^{\alpha N}\sum_{n'}^{\alpha N} a_n(\alpha)a_{n'}(\alpha)e^{-\beta\mathcal{F}_{N,M}(n,n',\tilde{R})}, \tag{16}$$

where one can distinguish three different cases: (a) $M = N$, $\alpha = 2$, the fully symmetric system (the macroions are identical, both with charge spanning the symmetric interval $[-Ne_0, Ne_0]$); (b) $M = N$, $\alpha > 2$, the semisymmetric system (the macroions are identical, both with charge spanning the asymmetric interval $[-Ne_0, \alpha Ne_0]$); and (c) $N \neq 0$, $M = 0$, $\alpha = 1$, the asymmetric system (one particle is positive, with charge fluctuating $[0, Ne_0]$, the other negative with charge spanning the interval $[-Ne_0, 0]$). The partition function (16) can be evaluated exactly only numerically, as we will do, in addition to providing two explicit analytical approximations.

III. SYMMETRIC-ASYMMETRIC CHARGES ON PROTEINS

With this we proceed to calculate the average value of the charge of the macroions $\langle e_{1,2}\rangle$, charge cross correlation $\langle e_1 e_2\rangle$, and autocorrelation function $\langle e_1 - \langle e_1\rangle\rangle^2$ for all three systems. The thermodynamic averages can be written as

$$\langle\cdots\rangle = \frac{1}{\mathcal{Z}}\sum_{n,n'}^{\alpha N} a_n(\alpha)a_{n'}(\alpha)\cdots e^{-\beta\mathcal{F}_{N,M}(n,n',\tilde{R})}. \tag{17}$$

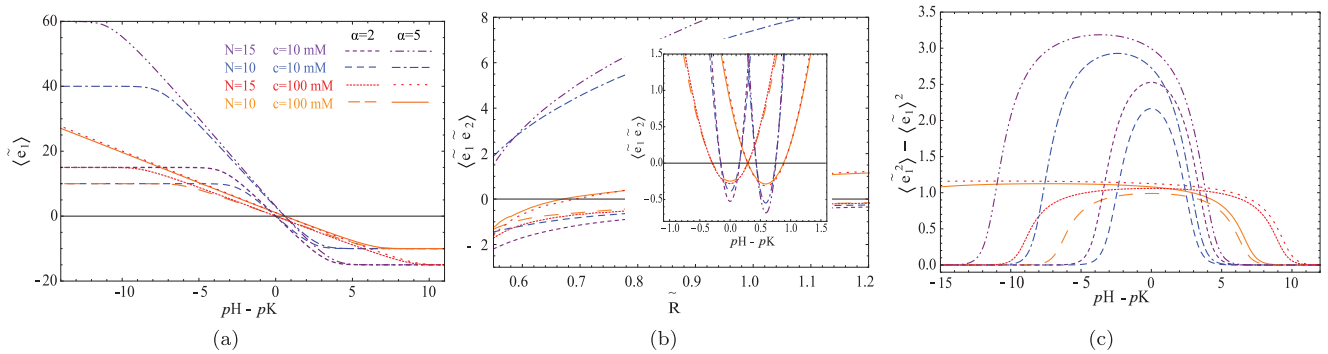

FIG. 2. (Color online) Symmetric system: (a) average charge of macroions, (b) charge cross-correlation function, and (c) autocorrelation function. All averages are obtained by exact evaluation of the partition function. Two systems are shown: a fully symmetric system with $\alpha = 2$ and the semisymmetric case, which takes the asymmetry coefficient to be $\alpha = 5$. Each line style corresponds to a choice of parameters (number of adsorption sites N and salt concentration c) and the system under consideration, as described in (a). The dimensionless diameter of the macroions is set to be $\tilde{a} = 0.5$ and the separation between them is $\tilde{R} = 1$. The $\tilde{R}$ dependence is plotted at the PZC $p\mathrm{H} - p\mathrm{K} = 0$.

In this way we can write, e.g., the dimensionless average charge of the particle $\langle \tilde{e}_1 \rangle = \langle e_1 \rangle / e_0$ as

$$\langle \tilde{e}_1 \rangle = \langle (n - M) \rangle. \tag{18}$$

In a similar way, other averages are calculated exactly from the full partition function and are plotted as functions of $\tilde{R}$ and $p\mathrm{H} - p\mathrm{K}$, for different values of the number of absorption sites N and salt concentration c, keeping fixed the diameter of the macroions $\tilde{a}$ (see Figs. 2 and 4).

In a fully symmetric system (Fig. 2, $\alpha = 2$), the average charge is allowed to vary in a symmetric interval, reaching the point of zero charge (PZC) for $p\mathrm{H} = p\mathrm{K}$. Away from the PZC, the average charge changes almost linearly until it reaches saturation and stays constant for any value of $p\mathrm{H} - p\mathrm{K}$ [Fig. 2(a)]. The charge cross-correlation function, being negative close to the PZC, indicates that even in the fully symmetric system the macroion charges tend to fluctuate asymmetrically, charge fluctuation on one macroion being accompanied by a fluctuation of the opposite sign on the other macroion [Fig. 2(b)]. This is a robust property of the system, fully discernible also in the one-dimensional exact solutions [22]. Considering the charge cross-correlation function as a function of distance between macroions, plotted for fixed $p\mathrm{H} - p\mathrm{K}$, one can observe that at the PZC, the fluctuation asymmetry effect decreases as separation increases and it is strongest for smaller values of salt concentration, while close to the PZC, the asymmetry appears in the regime of larger salt concentration and smaller separations. The charge autocorrelation function is positive with the maximum centered at the PZC, being bigger for smaller salt concentration [Fig. 2(c)].

Finally, the interaction force is calculated as

$$\tilde{F}(\tilde{R}) = -\frac{d}{d\tilde{R}}[-\ln \mathcal{Z}(\tilde{R})]$$

and is shown in Fig. 3. Two identical macroions repel for most values of the parameters, but show a net attraction in the vicinity of the PZC. This attraction is of purely fluctuational origin, stemming from the asymmetric charge cross correlation. At the same value of dimensionless separation, the strength of this fluctuation attraction is larger in systems with larger salt concentration and a larger number of adsorption sites.

Concerning the semisymmetric system of macroions with both charges spanning the same asymmetric interval (Fig. 2, $\alpha = 5$), one can discern similar behavior of all averages as in the fully symmetric system. However here, the PZC is no longer determined by $p\mathrm{H} = p\mathrm{K}$, but is shifted, meaning that the concentration of the positive ions close to the macroion surfaces is different from the concentration of protons in the bulk. The autocorrelation function as a function $p\mathrm{H} - p\mathrm{K}$ is not centered anymore on the PZC, but the asymmetric fluctuations do again appear at the PZC [Fig. 2(b)], where one can observe net attraction between the macroions (Fig. 3, inside graph).

The behavior of the completely asymmetric system is shown in Figs. 4 and 5. Here, away from the PZC, the first macroion is positive and the second neutral, or the first can be neutral while the second can be negatively charged, depending on the value of $p\mathrm{H} - p\mathrm{K}$. In the region $-3 \lessapprox p\mathrm{H} - p\mathrm{K} \lessapprox 3$

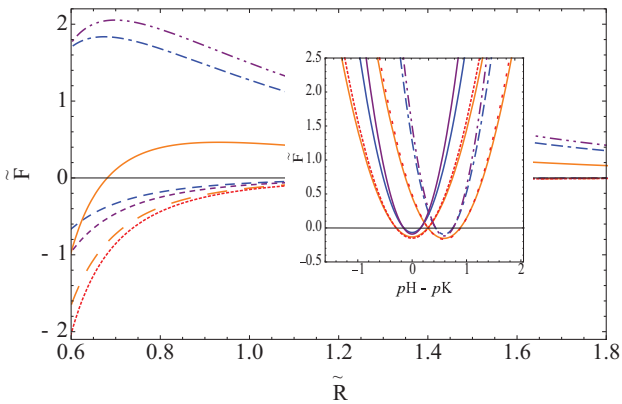

FIG. 3. (Color online) Interaction force for the fully symmetric system (solid lines) and the semisymmetric system (dashed lines). All averages are obtained by exact evaluation of the partition function. Each line style corresponds to a choice of parameters (number of adsorption sites N and salt concentration c) and the system under consideration, as described in Fig. 2(a). The $\tilde{R}$ dependence is plotted at the PZC $p\mathrm{H} - p\mathrm{K} = 0$, while the $p\mathrm{H} - p\mathrm{K}$ dependence is plotted setting by $\tilde{R} = 1$. The dimensionless diameter of the macroions is taken to be $\tilde{a} = 0.5$.

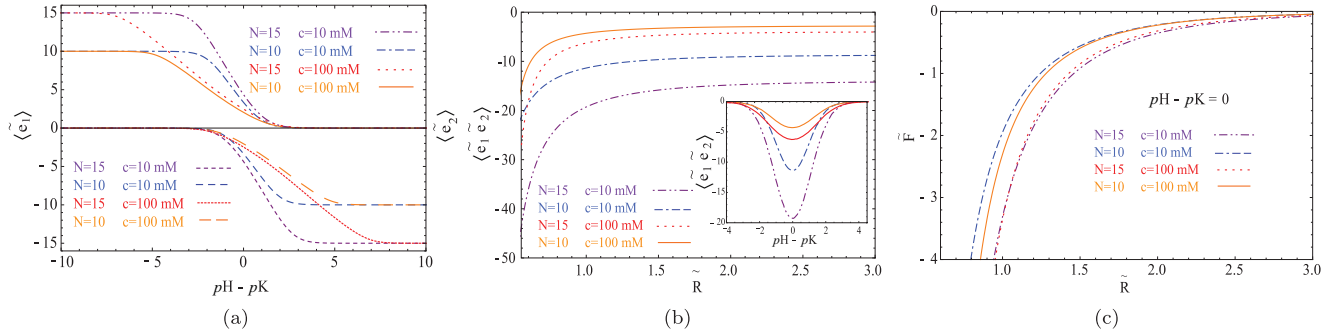

FIG. 4. (Color online) Asymmetric system: (a) average charge of macroions, (b) charge cross-correlation function, and (c) interaction force. All averages are obtained using the exact evaluation of the full partition function. Each line style corresponds to a choice of parameters (number of adsorption sites N and salt concentration c) as described in the legend. The dimensionless diameter of the macroions is set to be $\tilde{a} = 0.5$ and the separation between them is $\tilde{R} = 1$. The $\tilde{R}$ dependence is plotted at a point determined with $p\mathrm{H} - p\mathrm{K} = 0$.

both macroions carry nonzero charge of opposite sign and at $p\mathrm{H} = p\mathrm{K}$ the system is electroneutral as a whole, i.e., the sum of average charges is equal to zero [Fig. 4(a)]. The charge cross-correlation function is always negative [Fig. 4(b)] and one can observe only attraction [Fig. 4(c)]. The number of adsorption sites has the biggest influence on the intensity of the interaction.

The fluctuation effect shows an interesting twist in this system: The interaction force as a function of separation shows attraction also when one of the macroions is charged and the other reaches its point of zero charge [see Fig. 5(a)]. The origin of that attraction comes from the mean charge-induced charge interaction [see Fig. 5(b)], where one can observe a nonzero product $\langle \tilde{e}_i \rangle^2$ ($\langle \tilde{e}_j - \langle \tilde{e}_j \rangle \rangle^2$) of nonzero charge $\langle \tilde{e}_i \rangle^2$ and autocorrelation function of zero charge $\langle \tilde{e}_j \rangle$. As is the case in the symmetric system, here also for the same dimensionless separation the attraction is significantly stronger in a solution with larger salt concentration.

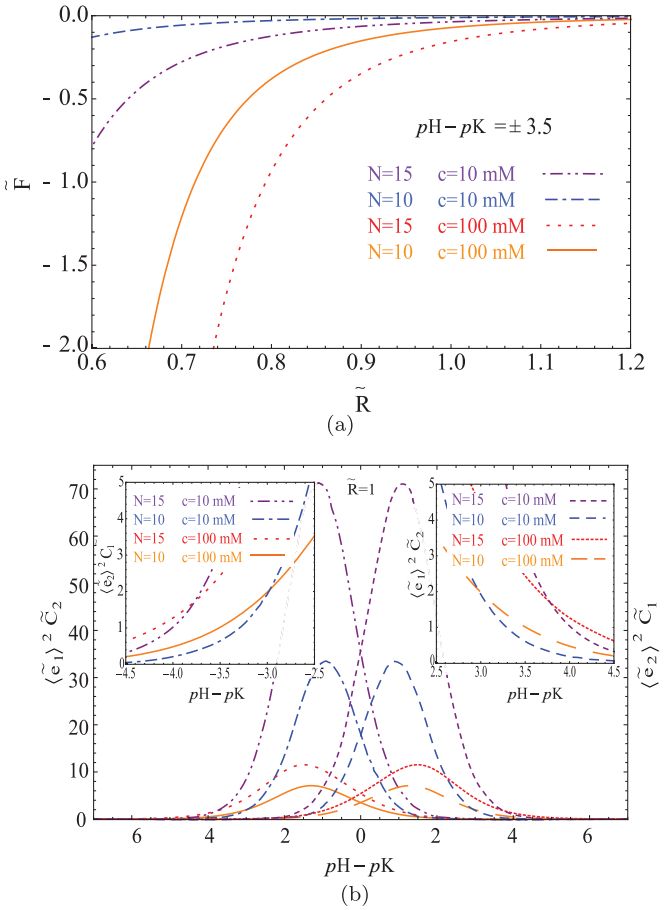

FIG. 5. (Color online) Asymmetric system: (a) interaction force plotted at $p\mathrm{H} - p\mathrm{K} = 3.5$ and (b) $\langle \tilde{e}_1 \rangle^2 \langle \tilde{e}_2 - \langle \tilde{e}_2 \rangle \rangle^2$ and $\langle \tilde{e}_2 \rangle^2 \langle \tilde{e}_1 - \langle \tilde{e}_1 \rangle \rangle^2$. All averages are obtained using the exact evaluation of the full partition function. Each line style corresponds to a choice of parameters (number of adsorption sites N and salt concentration c) as described in the legend. The dimensionless diameter of the macroions is set to be $\tilde{a} = 0.5$.

IV. DISCUSSION

In the previous section we showed results obtained numerically using the exact evaluation of the full partition function. The aim of this section is to seek an analytical approximation that will provide better intuition about the behavior of the attractive interaction arising between identical macroions with fluctuating charge so that it can be compared with the original KS result for the attractive components as well as the DH result for the repulsive component, respectively. In order to do so, we will evaluate the partition function (16), introducing two different approximations, the saddle-point approximation and the Gaussian approximation, comparing the ensuing approximative results with the exact ones. The approximations refer to the evaluation of the partition function (4) and not to the evaluation of the field Green's function $G(\varphi_1,\varphi_2)$, which is always assumed to be of the DH form. All the approximations detailed below thus refer to the evaluation of the charge-regulation part of the partition function.

A. Saddle-point approximation

The saddle-point approximation consists of finding the dominant contribution to the partition function, corresponding to the minimum of the field action, which is then expanded around the minimum to the second order in deviation. The saddle-point approximation is usually referred to also as the mean-field approximation, but we need to distinguish the mean field in the treatment of the charge-regulation free

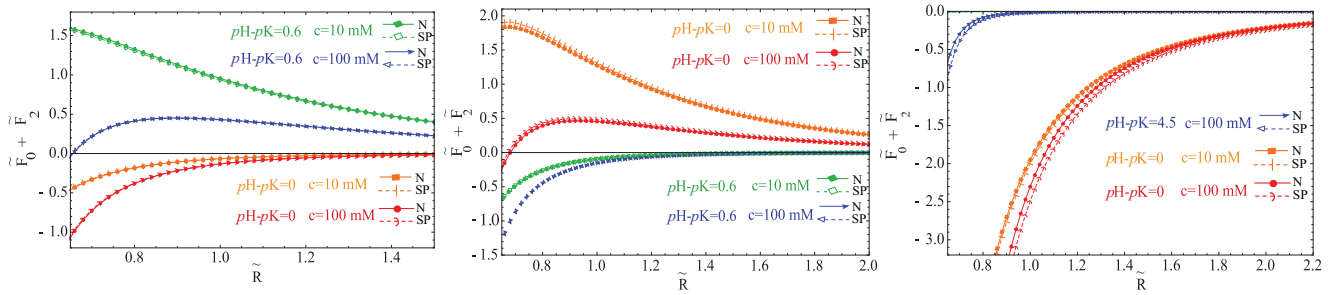

FIG. 6. (Color online) Total interaction force, obtained using the saddle-point approximation to evaluate the the full partition function (SP), compared with numerical results, obtained using the exact evaluation of the full partition function (N) for the (a) fully symmetric system with $\alpha = 2$, (b) semisymmetric system with $\alpha = 5$, and (c) asymmetric system. Each line style corresponds to a different choice of parameters (number of adsorption sites N, salt concentration c, and $p\mathrm{H} - p\mathrm{K}$) as indicated. The dimensionless diameter of the macroions is set to be $\tilde{a} = 0.5$.

energy with the PB mean field, which refers to the interaction part. The procedure is detailed in Appendix B, where we derive expressions for the saddle-point free energy, as well as the fluctuation-induced free energy from the second-order correction (B9). With respect to that decomposition, one can distinguish the saddle-point interaction force $\tilde{F}_0$ and the fluctuation component of the interaction force $\tilde{F}_2$ with magnitudes given as

$$\tilde{F}_0 = k\frac{1+\tilde{R}}{\tilde{R}^2}\tilde{a}^2 e^{2\tilde{a}-\tilde{R}} \times \frac{[\phi_1^* - (\tilde{a}/\tilde{R})e^{\tilde{a}-\tilde{R}}\phi_2^*][\phi_2^* - (\tilde{a}/\tilde{R})e^{\tilde{a}-\tilde{R}}\phi_1^*]}{[1-(\tilde{a}/\tilde{R})^2 e^{-2(\tilde{R}-\tilde{a})}]^2} \tag{19}$$

and

$$\tilde{F}_2 = -\frac{1+\tilde{R}}{\tilde{R}^3}\frac{\tilde{a}^2 e^{-2(\tilde{R}-\tilde{a})}}{h_1(\phi_1^*)h_2(\phi_2^*) - (\tilde{a}/\tilde{R})^2 e^{-2(\tilde{R}-\tilde{a})}}. \tag{20}$$

Here $k = \frac{4\pi\epsilon\epsilon_0}{\beta e_0^2 \kappa}$, while $h_1(\phi_1^*)$ and $h_2(\phi_2^*)$ are defined as

$$\begin{aligned} h_1(\phi_1^*) &= 1 + \frac{k\tilde{a}}{\alpha b N} e^{\tilde{a}} e^{-\phi_1^*}(b + e^{\phi_1^*})^2, \\ h_2(\phi_2^*) &= 1 + \frac{k\tilde{a}}{\alpha b N} e^{\tilde{a}} e^{-\phi_2^*}(b + e^{\phi_2^*})^2, \end{aligned} \tag{21}$$

with ϕ_1^* and ϕ_2^* the solutions of the saddle-point equations (B3) and (B4) given in Appendix B. Since they are obtained numerically, this method does not give us a transparent analytical solution for the free energy and interaction force.

The sum of the saddle-point interaction force $\tilde{F}_0$ and the fluctuation force $\tilde{F}_2$ for symmetric, semisymmetric, and asymmetric systems are plotted as functions of separation $\tilde{R}$ and compared with results obtained by exact evaluation of the full partition function (Fig. 6). One can notice that there is excellent agreement between both results obtained using these different methods. The saddle-point method decouples the total force into a saddle-point part and a fluctuation part, one being repulsive and the other attractive, respectively, except for the asymmetric system, where there is no repulsion whatsoever [Fig. 6(c)]. They can be differentiated based on the separation scaling of the interaction free energy. In the first case it decays exponentially with $\tilde{R}$, while in the second it decays exponentially with $2\tilde{R}$. The repulsive force decreases as the system approaches the PZC, where it is identically equal to zero. In this regime the fluctuation component to the interaction force becomes the dominant one.

The main and important difference between the interactions calculated exactly or on the saddle-point level is that the attractive component of the interaction force in the latter case does not depend on $p\mathrm{H}$, but is sensitive and increases with the salt concentration [Figs. 6(a) and 6(b)]. The full $p\mathrm{H}$ dependence of the interaction is thus not described properly by the saddle-point approximation.

B. Gaussian approximation

In this case the analytical evaluation of the partition function (16) is based on a Gaussian approximation for the binomial coefficient and is presented in Appendix C. The partition function in this case also decouples into two separate contributions, of which one decays exponentially with $\tilde{R}$ and the other decays exponentially with $2\tilde{R}$. We will again refer to them as the mean and the fluctuation part of the interaction force, using the same notation as for the saddle-point approximation. One should note here that on this approximation level there is no real decoupling into the mean and fluctuation part. We differentiate them purely based on their separation scaling.

The mean interaction force $\tilde{F}_0$ can be obtained as

$$\tilde{F}_0 = k\frac{1+\tilde{R}}{\tilde{R}^2}\tilde{a}^2 e^{2\tilde{a}-\tilde{R}}\frac{[(p\mathrm{H}-p\mathrm{K})\ln 10]^2}{[1+2(k\tilde{a}/N)e^{\tilde{a}} + (\tilde{a}/\tilde{R})e^{-(\tilde{R}-\tilde{a})}]^2} \tag{22}$$

and the fluctuation force $\tilde{F}_2$ as

$$\tilde{F}_2 = -\frac{1+\tilde{R}}{\tilde{R}^3}\frac{\tilde{a}^2 e^{-2(\tilde{R}-\tilde{a})}}{[1+(4k\tilde{a}/\alpha N)e^{\tilde{a}}]^2 - (\tilde{a}^2/\tilde{R}^2)e^{-2(\tilde{R}-\tilde{a})}}. \tag{23}$$

Again both $\tilde{F}_0$ and $\tilde{F}_2$ are obtained in the same way and the separation into mean and fluctuation parts is arbitrary. Nevertheless, the separation scaling of the two is the same as for the mean-field and fluctuation contributions in the case of the saddle-point approximation, making the nomenclature reasonable.

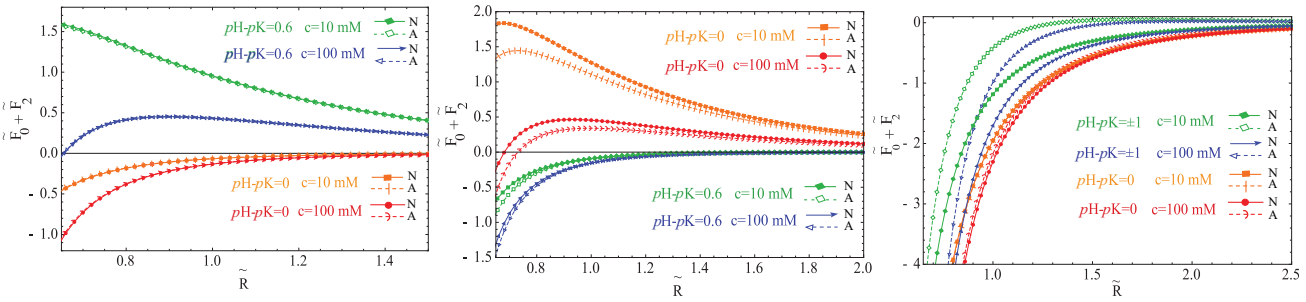

FIG. 7. (Color online) Analytical results for the total force, obtained using approximative evaluation of the full partition function (A), are compared with numerical results, obtained using exact evaluation of the full partition function (N) for the (a) fully symmetric system with $\alpha = 2$, (b) semisymmetric system with $\alpha = 5$, and (c) asymmetric system. Each line style corresponds to the choice of parameters (number of adsorption sites N, salt concentration c, and $p\mathrm{H} - p\mathrm{K}$) as indicated. The dimensionless diameter of the macroions is set to be $\tilde{a} = 0.5$.

The general form of the mean interaction force is given in Eq. (C4), which is valid for all three systems considered: fully symmetric, semisymmetric, and asymmetric. Because of its complexity, we display here only $\tilde{F}_0$ for the fully symmetric system (22). On the other hand, the fluctuation force (23) has the same universal form for all three types of systems. One can compare these results (22) and (23) with those obtained using the saddle-point approximation (19) and (20).

Clearly, the fluctuation force in the Gaussian approximation corresponds exactly to the fluctuating force in the saddle-point approximation if the saddle point is taken at the PZC $p\mathrm{H} = p\mathrm{K}$ and the mean potentials are $\phi_1^* = \phi_2^* = 0$. However, in general, the two approximations do not coincide and thus we cannot claim that $\tilde{F}_2$ is purely fluctuational in origin.

The mean and the fluctuation part to the interaction force are plotted as functions of dimensionless separation $\tilde{R}$ in Fig. 7. The total interaction force obtained in this way is compared with the one obtained using the exact evaluation of the partition function. For the fully symmetric system, the Gaussian approximation fits perfectly the exact results [Fig. 7(a)]. Somewhat lesser agreement can be found in a semisymmetric system [Fig. 7(b)], while the analytical results do not work at all in the region away from the PZC in the asymmetric system [Fig. 7(c)].

In the fully symmetric system, the mean part of the interaction force is repulsive, decreasing on approach to the PZC, while in the asymmetric system, it is actually attractive as the macroions are on average oppositely charged. On the other hand, the fluctuation component to the interaction force is attractive no matter what the symmetry of the system and the $p\mathrm{H}$ of solution are, while it does depend on the salt concentration. Interestingly enough, on the Gaussian approximation level for the binomial coefficient the $p\mathrm{H}$ dependence of the autocorrelation function again drops out completely, which is contrary to the full numerical evaluation of the charge autocorrelation function.

C. Comparison with DH and KS forms

We now set our results against the mean-field DH theory of interactions between pointlike macroions and against the KS theory of charge-fluctuation forces. Obviously, without charge regulation the charge of both interacting macroions is fixed and the DH form of the interaction should be recovered. Setting $\alpha = 0$ and $M = N$ in Eq. (16), one indeed gets the DH interaction force between two well-separated like-charged macroions in a salt solution

$$\tilde{F} \approx \frac{N^2}{k}\frac{e^{-\tilde{R}}}{\tilde{R}}. \tag{24}$$

Charge regulation, besides inducing attraction at the PZC, also introduces significant modifications in the mean-field interaction force (22), leading to its vanishing at the PZC. In the limit of large separations, the charge-regulated interaction force (22) in fact scales as

$$\tilde{F}_0 \approx \frac{1}{\tilde{R}} k\tilde{a}^2 e^{2\tilde{a}-\tilde{R}} \frac{[(p\mathrm{H} - p\mathrm{K})\ln 10]^2}{[1 + 2(k\tilde{a}/N)e^{\tilde{a}}]^2}, \tag{25}$$

clearly showing a strong dependence on the solution $p\mathrm{H}$.

As for the fluctuation component of the interaction force for two spherical pointlike macroions, we can cast its form in the Gaussian approximation, going to a limit of asymptotically large separation (23) as

$$\tilde{F}_2 \approx -\frac{1}{\tilde{R}^2}\frac{\tilde{a}^2 e^{-2(\tilde{R}-\tilde{a})}}{[1 + 2(k\tilde{a}/N)e^{\tilde{a}}]^2}. \tag{26}$$

In this limit the charge autocorrelation functions for the two macroions $\langle \Delta\tilde{e}_1^2 \rangle = \langle (\tilde{e}_1 - \langle \tilde{e}_1 \rangle)^2 \rangle$ are independent of the separation between them and can be calculated analytically using the same Gaussian approximation with the following result:

$$\langle \Delta\tilde{e}_1^2 \rangle \langle \Delta\tilde{e}_2^2 \rangle \approx \frac{k^2\tilde{a}^2 e^{2\tilde{a}}}{[1 + 2(k\tilde{a}/N)e^{\tilde{a}}]^2}. \tag{27}$$

With this result the fluctuation component of the interaction force assumes the asymptotic form

$$\tilde{F}_2 \approx -\frac{e^{-2\tilde{R}}}{k^2\tilde{R}^2}\langle \Delta\tilde{e}_1^2 \rangle \langle \Delta\tilde{e}_2^2 \rangle. \tag{28}$$

This actually coincides exactly with the original Kirkwood-Schumaker result [7,8] if we take into account the fact that they take the DH Green's function for two point charges with a finite-size scaling factor $e^{\tilde{a}}/(1 + \tilde{a})$, so that we would have to multiply Eq. (28) by $e^{-2\tilde{a}}(1 + \tilde{a})^2$. Again we note that on this approximation level the $p\mathrm{H}$ dependence of the autocorrelation function drops out completely, but is retained

TABLE I. The pK values of amino-acid functional groups in dilute aqueous solution, after Ref. [16].

AA	pK
Asp	3.71
Glu	4.15
Tyr	10.10
Arg	12.10
His	6.04
Lys	10.67
Cys	8.14

in the full numerical evaluation of the charge autocorrelation function.

V. PROTEINLIKE MACROIONS

The general theory formulated above can be straightforwardly applied to the interaction of proteinlike macroions. In a protein, the amino acids (AAs) Asp, Glu, Tyr, and Cys can be negatively charged, while Arg, Lys, and His can carry a positive charge, all depending on the solution conditions. The respective pK for the dissociation of the various amino acids are given at Table I [16].

In order to describe a protein macroion composed of these amino acids, one should write down the charge-regulation free energy in the form

$$f_p(\varphi) = i\sum_j N_j M_j e_0\varphi - kT\sum_j N_j M_j \ln\left(1 + b_j e^{i\beta e_0\varphi}\right) - kT\sum_k N_k M_k \ln\left(1 + b_k e^{i\beta e_0\varphi}\right), \tag{29}$$

where j stands for negative AAs $j = \{\text{Asp,Glu,Tyr,Cys}\}$, while k stands for positive ones $k = \{\text{Arg,His,Lys}\}$. Here N_j and N_k are the numbers of absorption sites on each positive AA and negative AA and since each of these AAs has one adsorption site it will be set to 1. In addition, M_j and M_k count how many times each AAs occurs in the protein and b_j and b_k stand for $b_n = e^{-\ln 10(p\text{H}-p\text{K}_n)}$, where the $p\text{K}_n$ for each AA is given in Table I. For pointlike macroions the spatial distribution of AAs on the surface of the protein is irrelevant and the above approximation is thus admissible.

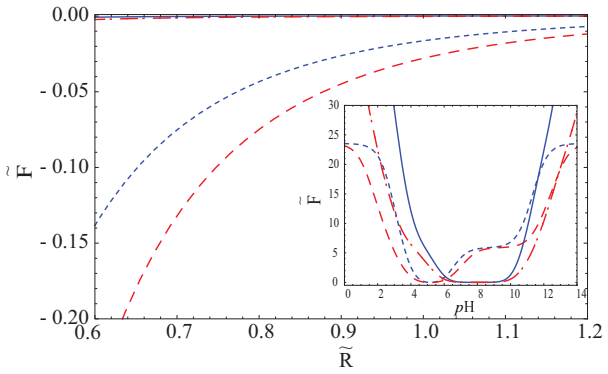

FIG. 9. (Color online) Generalized system: interaction force. All results are obtained by using the exact numerical evaluation of the full partition function. Each line style corresponds to a choice of system and the values of salt concentration c as indicated in Fig. 8(a). The functions bearing an $\tilde{R}$ dependence are plotted at the isoelectric point of the two systems: $p\text{H} = 5.15$ and 7.87, respectively. The dimensionless diameter of the macroions is set to be $\tilde{a} = 0.5$ and the separation between them is $\tilde{R} = 1$.

The partition function for the system composed of two proteinlike macroions in a 1:1 salt solution is derived in the same way as explained in Sec. II and is given in Appendix D. Since the evaluation of Eq. (D2) is computationally time consuming, we consider only the behavior of two model systems, one (system I) composed of proteinlike macroions consisting of two Asp, two Glu, two Lys, and two His AAs and the other (system II) having four AAs more, two Tyr and two Arg. The results are shown in Figs. 8 and 9. The protein charge, as a function of pH, spans a symmetric interval with constant plateaus in the pH regions, which correspond to charging up an additional AA. The cross-correlation function in general follows the pattern of plateaus of the average charge, being positive everywhere except at the PZC, where an asymmetric charge distribution appears. The autocorrelation function and

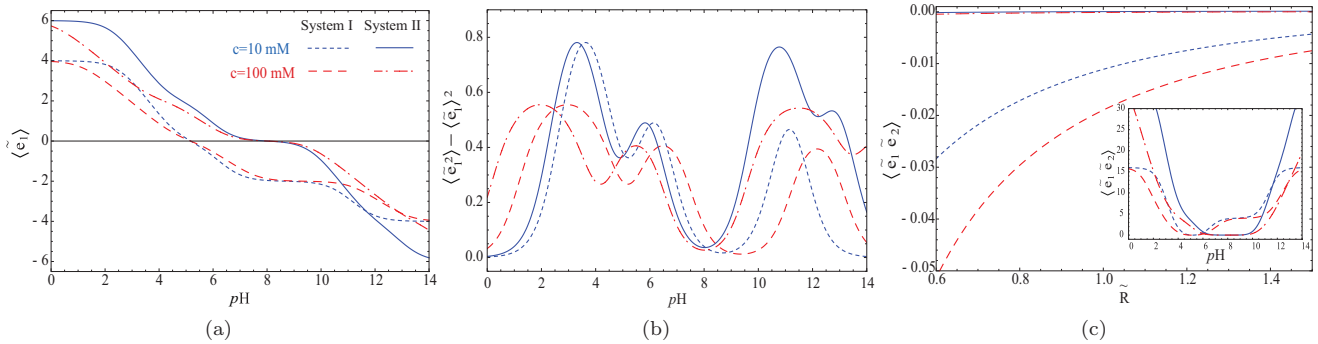

FIG. 8. (Color online) Generalized system: (a) average charge of macroions, (b) charge autocorrelation function, and (c) charge-charge cross-correlation function. All results are obtained by using the exact numerical evaluation of the full partition function. System I consists of two proteins, each of which consists of 2 Asp, 2 Glu, 2 Lys, and 2 His AAs, while system II has additional 2 Tyr and 2 Arg. The results are plotted for two different values of salt concentration $c = 10$ and 100 mM for each system. The dimensionless diameter of the macroions is set to be $\tilde{a} = 0.5$ and the separation between them $\tilde{R} = 1$. The functions bearing an $\tilde{R}$ dependence are plotted at the isoelectric point of the two systems: $p\text{H} = 5.15$ and 7.87, respectively.

the charge cross correlation show opposite signs, with one being positive and the other negative, respectively.

Analyzing the behavior of the interaction force Fig. 9, one can see that two identical proteins mutually repel and that the strength of the interaction depends on the pH in the solution, following closely the behavior of the charge cross-correlation function. The repulsion is smaller in a solution of higher salt concentration, since the salt screens the protein charge and reduces the interaction. The repulsion disappears at the PZC, where the attraction sets in, increasing with salt concentration at a fixed dimensionless separation between the proteins. The attractive interaction is negligible for proteins composed of a larger number of amino acids, which does not correspond with our previous results, where the attraction is larger for a larger number of adsorption sites. This can be explained by analyzing the average charge of the protein [Fig. 8 (a)], where one can observe a plateau of zero charge for system II, which is not the case in system I. So it can be concluded that the strength of the fluctuation interaction depends on the rate of change of the charge of the macroion with pH, which of course depends on the type of the protein.

This can be derived also formally by following Lund and Jönsson [11]. The fluctuation part of the interaction force (28) is approximately proportional to the charge variance, which in turn follows from the macroion capacitance $\mathcal{C}$ as

$$\langle(\tilde{e} - \langle\tilde{e}\rangle)^2\rangle \sim \mathcal{C} = \frac{\partial\tilde{e}(\phi)}{\partial(\beta e_0\phi)} = -\frac{1}{\ln 10}\frac{\partial\tilde{e}(\phi)}{\partial p\mathrm{H}}, \qquad (30)$$

as is clear also from Eq. (3). The strength of the fluctuation interaction therefore depends on the rate of change of the mean charge of the macroion with pH, i.e., its capacitance. This can be clearly discerned from Fig. 8(b), where we observe that system II has zero capacitance at its PZC, while system I has a nonzero capacitance at its PZC.

VI. CONCLUSION

We presented a theory describing electrostatic interaction between two spherical macroions, with nonconstant, fluctuating charge, surrounded by a monovalent bathing salt solution. The macroion charge fluctuations are described with the Parsegian-Ninham model of charge regulation, which effectively corresponds to a lattice-gas surface dissociation free energy. Our theory is based on two approximations: One assumes the macroions as pointlike, in the sense that the electrostatic potential on the surface of the macroion is uniform, and other treats the intervening salt solution on the Debye-Hückel level, assuming the electrostatic potential to be small, so that the Poisson-Boltzmann equation can be linearized. Choosing the proper charge-regulation energy, we analyzed the behavior of three different systems that differ in the symmetry of charge distribution. These are a symmetric system composed of two identical macroions with a symmetric as well as asymmetric charge-regulation intervals, corresponding to the fully symmetric and semisymmetric cases, and an asymmetric system, composed of oppositely charged macroions, allowing the case of having one charged and one uncharged particle.

We have shown that in charge-regulated systems, asymmetrical charge fluctuations appear near the PZC, engendering strong attractive interactions of a general Kirkwood-Schumaker type, but with different functional dependences as argued in their original derivation. The fluctuational nature of the Kirkwood-Schumaker interaction is consistent also with the fact that it arises even between a charged and a charge neutral object, in the vicinity of the pH where the charged macroion becomes neutral itself. This is the case studied also in the context of the PB theory within the constant charge-regulation model, in fact corresponding to a linearized form of the full charge-regulation theory [24,25]. In this limit too the effects of charge regulation are crucial and lead to attraction. However, in the context of our approximations, the attractive interaction between a charged and a neutral surface stems from the coupling between the net charge of one and charge fluctuations of the other surface. Superficially, one would tend to see the attraction in the constant charge-regulation model as being grounded in the mean-field level, but caution should be exercised here. In our case too the Green's function pertains to the DH mean-field level and the attraction actually comes from the surface charge regulation. The constant-charge-regulation model must obviously capture some of the same physics.

The bathing solution with its pH and ionic strength therefore plays an important role in charge-regulated systems and the interactions to which they are subject. In all cases studied, the fluctuation attraction is larger for larger salt concentration in solution at the same dimensionless separation, while the repulsion is actually reduced at a fixed separation by increasing the salt concentration, consistent with the electrolyte screening effect. Furthermore, a stronger attraction is found in systems composed of identical macroions having a larger number of adsorption sites, giving rise to larger charge fluctuations.

The theory, developed for toy models, was then applied to the case of proteinlike macroions, with a different dissociation constant for different chargeable amino acids. For protein electrostatic interactions their strength depends on the rate of change of the charge of the macroion with respect to the solution pH, i.e., the molecular capacitance of the macroion, which is protein specific and connected with the capacitance of the protein charge distribution. Apart from this, salt concentration enhances the attraction between proteinlike macroions, as evidenced also in simulations and experiments in the case of, e.g., lysozyme in monovalent salt solutions [26,27]. In fact, understanding the details of the protein-protein interaction is our main motivation for developing further our theoretical approach, specifically the relation between the KS interaction, the patchiness effects, and van der Waals interactions between proteins in electrolyte solutions.

ACKNOWLEDGMENTS

N.A. acknowledges financial support from the Slovenian Research Agency under the young researcher grant. R.P. acknowledges financial support from the Slovenian Research Agency under Grant No. P1-0055 and would like to thank Professor Michal Borkovec and Dr. Gregor Trefalt for illuminating discussions on the subject of charge regulation and electrostatic interactions between charge-regulated macroions.

APPENDIX A: PATH-INTEGRAL FORMALISM

The field propagator at points $\vec{r}_1$ and $\vec{r}_2$ is defined as

$$G(\varphi_1,\varphi_2)=\int_{\varphi(\vec{r}_1)=\varphi_1}^{\varphi(\vec{r}_2)=\varphi_2}\mathcal{D}[\varphi(\vec{r}\,)]\delta(\varphi(\vec{r}_1)-\varphi_1)\delta(\varphi(\vec{r}_2)-\varphi_2)\exp\left[-\frac{1}{2}\int d\vec{r}\,d\vec{r}\,'\varphi(\vec{r}\,)G^{-1}(\vec{r},\vec{r}\,)\varphi(\vec{r}\,')\right], \tag{A1}$$

where $G^{-1}(\vec{r},\vec{r}\,')$ is the usual Debye-Hückel kernel of the form [4]

$$G^{-1}(\vec{r},\vec{r}\,')=-\varepsilon_0[\vec{\nabla}\varepsilon(\vec{r}\,)\vec{\nabla}-\varepsilon(\vec{r}\,)\kappa^2]\delta(\vec{r}-\vec{r}\,'), \tag{A2}$$

where κ is the inverse Debye length. Using the δ function in the integral representation

$$\delta(\varphi(\vec{r}_1)-\varphi_1)=\int\frac{dk}{2\pi}e^{ik[\varphi(\vec{r}_1)-\varphi_1]}=\int\frac{dk}{2\pi}\exp\left(-ik\varphi_1+ik\int d\vec{r}\rho_1(\vec{r}\,)\varphi(\vec{r}\,)\right), \tag{A3}$$

where $\rho_1(\vec{r}\,)=\delta(\vec{r}-\vec{r}_1)$, one can rewrite the propagator as

$$G(\varphi_1,\varphi_2)=\int dk\,e^{-ik\varphi_1}\int dk'e^{-ik'\varphi_2}\int\mathcal{D}[\varphi(\vec{r})]\exp\left[-\frac{1}{2}\int d\vec{r}\,d\vec{r}\,'\varphi(\vec{r}\,)G^{-1}(\vec{r},\vec{r}\,)\varphi(\vec{r}\,')+i\int t(\vec{r}\,)\varphi(\vec{r}\,)d^3\vec{r}\right], \tag{A4}$$

where $t(\vec{r}\,)$ stands for $t(\vec{r}\,)=k\rho_1(\vec{r}\,)+k'\rho_2(\vec{r}\,)$. After integration over the field, one obtains

$$\begin{aligned}G(\varphi_1,\varphi_2)&=\frac{1}{\det G^{-1}(\vec{r},\vec{r}\,')}\int dk\,e^{-ik\varphi_1}\int dk'e^{-ik'\varphi_2}\exp\left(-\frac{1}{2}\int d\vec{r}\,d\vec{r}\,'t(\vec{r}\,)G(\vec{r},\vec{r}\,')t(\vec{r}\,')\right)\\&=\frac{1}{\det G^{-1}(\vec{r},\vec{r}\,')}\int_{-\infty}^{+\infty}\int_{-\infty}^{+\infty}dk\,dk'e^{-ik\varphi_1-ik'\varphi_2}e^{-k^2G(\vec{r}_1,\vec{r}_1)/2}e^{-k'^2G(\vec{r}_2,\vec{r}_2)/2}e^{-kk'G(\vec{r}_1,\vec{r}_2)}.\end{aligned} \tag{A5}$$

If one introduces a two-dimensional vector $(k\,k')$, this integral can be rewritten as

$$G(\varphi_1,\varphi_2)=\frac{1}{\det G^{-1}(\vec{r},\vec{r}\,')}\int\int dk\,dk'\exp\left[-i\begin{pmatrix}\varphi_1\\\varphi_2\end{pmatrix}^T\begin{pmatrix}k\\k'\end{pmatrix}\right]\exp\left[-\frac{1}{2}\begin{pmatrix}k\\k'\end{pmatrix}^T\begin{pmatrix}G(\vec{r}_1,\vec{r}_1)&G(\vec{r}_1,\vec{r}_2)\\G(\vec{r}_1,\vec{r}_2)&G(\vec{r}_2,\vec{r}_2)\end{pmatrix}\begin{pmatrix}k\\k'\end{pmatrix}\right]. \tag{A6}$$

Since this is a Gaussian integral, it can be evaluated explicitly

$$G(\varphi_1,\varphi_2)=\exp\left[-\frac{\beta}{2}\begin{pmatrix}\varphi_1\\\varphi_2\end{pmatrix}^T\begin{pmatrix}G(\vec{r}_1,\vec{r}_1)&G(\vec{r}_1,\vec{r}_2)\\G(\vec{r}_1,\vec{r}_2)&G(\vec{r}_2,\vec{r}_2)\end{pmatrix}^{-1}\begin{pmatrix}\varphi_1\\\varphi_2\end{pmatrix}\right]. \tag{A7}$$

APPENDIX B: SADDLE-POINT APPROXIMATION

The partition function (4) can be evaluated using the saddle-point method, consisting of minimization of the field action $\frac{\partial A}{\partial\phi}=0$, where the action can be written in the form

$$A(\phi_1,\phi_2)=f_1(\phi_1)+g(\phi_1,\phi_2)+f_2(\phi_2), \tag{B1}$$

with g the logarithm of the Green's function, given as

$$g(\phi_1,\phi_2)=-\frac{1}{2}\begin{pmatrix}\phi_1\\\phi_2\end{pmatrix}^T\begin{pmatrix}\tilde{G}(\vec{r}_1,\vec{r}_1)&\tilde{G}(\vec{r}_1,\vec{r}_2)\\\tilde{G}(\vec{r}_1,\vec{r}_2)&\tilde{G}(\vec{r}_2,\vec{r}_2)\end{pmatrix}^{-1}\begin{pmatrix}\phi_1\\\phi_2\end{pmatrix}. \tag{B2}$$

The saddle-point equations are obtained as

$$N-\alpha N\frac{be^{-\phi_1}}{1+be^{-\phi_1}}+\phi_1\frac{4\pi\epsilon\epsilon_0}{\beta e_0^2\kappa}\frac{1}{e^{-2\tilde{a}}/\tilde{a}^2-e^{-2\tilde{R}}/\tilde{R}^2}\frac{e^{-\tilde{a}}}{\tilde{a}}-\phi_2\frac{4\pi\epsilon\epsilon_0}{\beta e_0^2\kappa}\frac{1}{e^{-2\tilde{a}}/\tilde{a}^2-e^{-2\tilde{R}}/\tilde{R}^2}\frac{e^{-\tilde{R}}}{\tilde{R}}=0, \tag{B3}$$

$$M-\alpha N\frac{be^{-\phi_2}}{1+be^{-\phi_{1/2}}}+\phi_2\frac{4\pi\epsilon\epsilon_0}{\beta e_0^2\kappa}\frac{1}{e^{-2\tilde{a}}/\tilde{a}^2-e^{-2\tilde{R}}/\tilde{R}^2}\frac{e^{-\tilde{a}}}{\tilde{a}}-\phi_1\frac{4\pi\epsilon\epsilon_0}{\beta e_0^2\kappa}\frac{1}{e^{-2\tilde{a}}/\tilde{a}^2-e^{-2\tilde{R}}/\tilde{R}^2}\frac{e^{-\tilde{R}}}{\tilde{R}}=0. \tag{B4}$$

Solutions of these equations are denoted by ϕ_1^* and ϕ_2^*. If one sets $M=0$ and $\alpha=1$, one deals with an asymmetric system, for $M=N$ and $\alpha=2$, one deals with a fully symmetric system, and the choice $M=N$ and $\alpha>2$ defines a symmetric system with an asymmetric interval of fluctuating charge, i.e., a semisymmetric system.

The action can be expanded around the SP solution up to the second order in deviation from ϕ_1^* and ϕ_2^*, yielding

$$A(\phi_1,\phi_2)=f_1(\phi_1^*)+g(\phi_1^*,\phi_2^*)+f_2(\phi_2^*)+\frac{1}{2}\frac{\partial^2A(\phi_1,\phi_2)}{\partial\phi_1^2}\bigg|_{\phi_1^*,\phi_2^*}\delta\phi_1^2+\frac{\partial^2A(\phi_1,\phi_2)}{\partial\phi_1\partial\phi_2}\bigg|_{\phi_1^*,\phi_2^*}\delta\phi_1\delta\phi_2+\frac{1}{2}\frac{\partial^2A(\phi_1,\phi_2)}{\partial\phi_2^2}\bigg|_{\phi_1^*,\phi_2^*}\delta\phi_2^2, \tag{B5}$$

where $f_{1/2}(\phi^*_{1/2})$ are given as

$$f_{1/2}(\phi^*_{1/2}) = -M\phi^*_{1/2} - \alpha N \ln(1 + be^{-\phi^*_{1/2}}). \tag{B6}$$

If we denote second derivatives in the equation above by A_{11}, A_{12}, and A_{22}, respectively, we have

$$\begin{aligned} A_{11} &= -\alpha N b \frac{e^{-\phi^*_1}}{(1+be^{-\phi^*_1})^2} - \frac{4\pi\epsilon\epsilon_0}{\beta e_0^2\kappa}\frac{1}{e^{-2\tilde{a}}/\tilde{a}^2 - e^{-2\tilde{R}}/\tilde{R}^2}\frac{e^{-\tilde{a}}}{\tilde{a}}, \\ A_{22} &= -\alpha N b \frac{e^{-\phi^*_2}}{(1+be^{-\phi^*_2})^2} - \frac{4\pi\epsilon\epsilon_0}{\beta e_0^2\kappa}\frac{1}{e^{-2\tilde{a}}/\tilde{a}^2 - e^{-2\tilde{R}}/\tilde{R}^2}\frac{e^{-\tilde{a}}}{\tilde{a}}, \\ A_{12} &= \frac{4\pi\epsilon\epsilon_0}{\beta e_0^2\kappa}\frac{1}{\frac{e^{-2\tilde{a}}}{\tilde{a}^2} - \frac{e^{-2\tilde{R}}}{\tilde{R}^2}}\frac{e^{-\tilde{R}}}{\tilde{R}}, \end{aligned} \tag{B7}$$

so the saddle point and the fluctuation free energy are equal to

$$\beta\mathcal{F}_0 = -[f_1(\phi^*_1) + g(\phi^*_1,\phi^*_2) + f_2(\phi^*_2)] \tag{B8}$$

and

$$\beta\mathcal{F}_2 = -\ln\frac{\det A_0}{\det A}, \tag{B9}$$

where A_0 is a matrix, related to the partition function of the unperturbed system, with the elements

$$\begin{aligned} A^0_{11} &= \frac{\partial^2 A_0(\phi_1,\phi_2)}{\partial\phi_1^2} = -\frac{4\pi\epsilon\epsilon_0}{\beta e_0^2\kappa}\frac{1}{e^{-2\tilde{a}}/\tilde{a}^2 - e^{-2\tilde{R}}/\tilde{R}^2}\frac{e^{-\tilde{a}}}{\tilde{a}}, \\ A^0_{22} &= \frac{\partial^2 A_0(\phi_1,\phi_2)}{\partial\phi_2^2} = -\frac{4\pi\epsilon\epsilon_0}{\beta e_0^2\kappa}\frac{1}{e^{-2\tilde{a}}/\tilde{a}^2 - e^{-2\tilde{R}}/\tilde{R}^2}\frac{e^{-\tilde{a}}}{\tilde{a}}, \\ A^0_{12} &= \frac{\partial^2 A_0(\phi_1,\phi_2)}{\partial\phi_1\partial\phi_2} = \frac{4\pi\epsilon\epsilon_0}{\beta e_0^2\kappa}\frac{1}{e^{-2\tilde{a}}/\tilde{a}^2 - e^{-2\tilde{R}}/\tilde{R}^2}\frac{e^{-\tilde{R}}}{\tilde{R}}. \end{aligned} \tag{B10}$$

Finally, the saddle-point interaction force and the force due to the fluctuations around the saddle point are given as

$$\tilde{F}_0 = \frac{4\pi\epsilon\epsilon_0}{\beta e_0^2\kappa}\frac{1+\tilde{R}}{\tilde{R}^2}\tilde{a}^2 e^{2\tilde{a}-\tilde{R}}\frac{[\phi^*_1 - (\tilde{a}/\tilde{R})e^{\tilde{a}-\tilde{R}}\phi^*_2][\phi^*_2 - (\tilde{a}/\tilde{R})e^{\tilde{a}-\tilde{R}}\phi^*_1]}{[1-(\tilde{a}/\tilde{R})^2 e^{-2(\tilde{R}-\tilde{a})}]^2}, \tag{B11}$$

$$\tilde{F}_2 = -\frac{1+\tilde{R}}{\tilde{R}^3}\frac{\tilde{a}^2 e^{-2(\tilde{R}-\tilde{a})}}{h_1(\phi^*_1)h_2(\phi^*_2) - (\tilde{a}^2/\tilde{R}^2)e^{-2(\tilde{R}-\tilde{a})}}, \tag{B12}$$

where

$$h_1(\phi^*_1) = 1 + \frac{4\pi\epsilon\epsilon_0\tilde{a}}{\beta e_0^2\kappa N\alpha b}e^{\tilde{a}}e^{-\phi^*_1}(b+e^{\phi^*_1})^2, \quad h_2(\phi^*_2) = 1 + \frac{4\pi\epsilon\epsilon_0\tilde{a}}{\beta e_0^2\kappa N\alpha b}e^{\tilde{a}}e^{-\phi^*_2}(b+e^{\phi^*_2})^2. \tag{B13}$$

The saddle point and the fluctuation force are plotted as functions of dimensionless separation $\tilde{R}$ in Fig. 6.

APPENDIX C: GAUSSIAN APPROXIMATION

The partition function (16) can be evaluated analytically if one takes a Gaussian approximation for the binomial coefficient

$$\binom{\alpha N}{n} = \frac{2^{\alpha N}}{\sqrt{\pi\alpha N/2}}e^{-(\alpha N-2n)^2/2\alpha N}. \tag{C1}$$

After the substitutions $x = \alpha N - 2n$ and $x' = \alpha M - 2n'$, summation can be transformed into the integral, when one assumes $N \gg 1$, so the partition function becomes

$$\mathcal{Z} = \int_{-\infty}^{\infty} dx \int_{-\infty}^{\infty} dx' e^{(1/2)(x+x')(p\mathrm{H}-p\mathrm{K})\ln 10} e^{-(1/2\alpha N)(x^2+x'^2)} e^{-\beta\mathcal{F}(x,x',\tilde{R})}, \tag{C2}$$

where

$$\mathcal{F}(x,x',\tilde{R}) = \frac{e_0^2\kappa}{8\pi\epsilon\epsilon_0}\left(\frac{e^{-\kappa a}}{a}\{[x+N(2-\alpha)]^2 + [x'+M(2-\alpha)]^2\} + 2\frac{e^{-\kappa R}}{R}[x+N(2-\alpha)][x'+M(2-\alpha)]\right). \tag{C3}$$

This is a general Gaussian-type integral and can be calculated analytically, but since the solution is too cumbersome, it is not displayed here. The interaction force then follows as a sum of the mean contribution to the force and the fluctuation force as

$$\tilde{F}_0 = k\tilde{a}^2 e^{2\tilde{a}-\tilde{R}} \frac{1+\tilde{R}}{\tilde{R}^2} \frac{[(p\mathrm{H}-p\mathrm{K})\ln 10]^2}{\{1+2(k\tilde{a}/N)e^{\tilde{a}}+(\tilde{a}/\tilde{R})e^{-(\tilde{R}-\tilde{a})}\}^2} + \frac{(\alpha-2)k\tilde{a}^2 e^{2\tilde{a}-\tilde{R}}}{\alpha^2 N[1+(4k\tilde{a}e^{\tilde{a}}/\alpha N)]^2} \frac{1+\tilde{R}}{\tilde{R}^2}$$
$$\times\left(-\frac{2\alpha(N+M)(p\mathrm{H}-p\mathrm{K})\ln 10}{(1+\{1/[1+(4k\tilde{a}e^{\tilde{a}}/\alpha N)]^2\}(\tilde{a}/\tilde{R})e^{-(\tilde{R}-\tilde{a})})^2} + \frac{4\alpha M(\alpha N-1)(p\mathrm{H}-p\mathrm{K})\ln 10[1/1+(4k\tilde{a}e^{\tilde{a}}/\alpha N)]e^{-(\tilde{R}-\tilde{a})}}{(1-\{1/[1+(4k\tilde{a}e^{\tilde{a}}/\alpha N)]^2\}(\tilde{a}^2/\tilde{R}^2)e^{-2(\tilde{R}-\tilde{a})})^2}\right.$$
$$\left.+\frac{(4\alpha M-8)(1+\{1/[1+(4k\tilde{a}e^{\tilde{a}}/\alpha N)]^2\}(\tilde{a}^2/\tilde{R}^2)e^{-2(\tilde{R}-\tilde{a})})-(\alpha-2)[1+\alpha(M^2/N^2)][4N/1+(4k\tilde{a}e^{\tilde{a}}/\alpha N)](\tilde{a}/\tilde{R})e^{-(\tilde{R}-\tilde{a})}}{(1-\{1/[1+(4k\tilde{a}e^{\tilde{a}}/\alpha N)]^2\}(\tilde{a}^2/\tilde{R}^2)e^{-2(\tilde{R}-\tilde{a})})^2}\right),$$
$$\tilde{F}_2 = -\frac{1+\tilde{R}}{\tilde{R}^3} \frac{\tilde{a}^2 e^{-2(\tilde{R}-\tilde{a})}}{\left[1+(4/\alpha)\left(4\pi\epsilon\epsilon_0\tilde{a}/\beta e_0^2\kappa N\right)e^{\tilde{a}}\right]^2-(\tilde{a}^2/\tilde{R}^2)e^{-2(\tilde{R}-\tilde{a})}}. \tag{C4}$$

The mean contributions to the force and fluctuation force are plotted as functions of separation $\tilde{R}$ and the results are presented in Fig. 7. We note that the nomenclature "mean" and "fluctuation" do not have the same meaning in the context of the Gaussian approximation as they do in the saddle-point approximation. In fact, in the former the interaction free energy cannot be consistently separated into mean and fluctuation types. We use this separation based on the dimensionless separation scaling.

APPENDIX D: PROTEINLIKE MACROIONS

The partition function for the system of two pointlike proteins immersed in monovalent salt solution and containing seven types of dissociable AAs, negatively charged {Asp,Glu,Tyr,Cys} and positively charged {Arg,His,Lys}, can be written as

$$\mathcal{Z}=\prod_{\ell=1,7}\sum_{i_\ell,i'_\ell}^{M_i^\ell,M_{i'}^\ell} b_\ell^{i_\ell+i'_\ell}\frac{M_i^\ell!}{i_\ell!(M_i^\ell-i_\ell)!}\frac{M_{i'}^\ell!}{i'_\ell!(M_{i'}^\ell-i'_\ell)!}e^{-\beta\mathcal{F}_{pp}}, \tag{D1}$$

where ℓ runs through {Asp,Glu,Tyr,Cys} and {Arg,His,Lys}, with

$$\mathcal{F}_{pp}=\frac{e_0^2\kappa}{8\pi\epsilon\epsilon_0}\left[\frac{e^{-\tilde{a}}}{\tilde{a}}\left(\sum_m\left(M_i^m-i\right)^2+\sum_m\left(M_{i'}^m-i'\right)^2\right)\right.$$
$$\left.+2\frac{e^{-\tilde{R}}}{\tilde{R}}\sum_m\left(M_i^m-i\right)\sum_m\left(M_{i'}^m-i'\right)\right], \tag{D2}$$

where the unprimed and the primed notation refer to the two protein macroions. Here M_i^ℓ counts how many times each of these seven amino acids occurs in a protein, while M_i^m is restricted to counting only negative amino acids. In addition, b_ℓ refers to the chemical energy of dissociation $b_\ell = e^{-\ln 10(p\mathrm{H}-p\mathrm{K}_\ell)}$, where the intrinsic $p\mathrm{K}_\ell$ for the seven dissociable amino acids are given in Table I.

[1] R. Piazza, Curr. Opin. Colloid Interface Sci. **8**, 515 (2004).
[2] T. Simonson, Rep. Prog. Phys. **66**, 737 (2003).
[3] D. Leckband and S. Sivasankar, Colloids Surf. B **14**, 83 (1999).
[4] A. Naji, M. Kanduč, J. Forsman, and R. Podgornik, J. Chem. Phys. **139**, 150901 (2013).
[5] N. I. Lebovka, Adv. Polym. Sci. **255**, 57 (2014).
[6] M. Borkovec, B. Jönsson, and G. J. M. Koper, Surf. Colloid Sci. **16**, 99 (2001).
[7] J. Kirkwood and J. B. Shumaker, Proc. Natl. Acad. Sci. USA **38**, 855 (1952).
[8] J. Kirkwood and J. B. Shumaker, Proc. Natl. Acad. Sci. USA **38**, 863 (1952).
[9] V. A. Parsegian, *Van der Waals Forces* (Cambridge University Press, Cambridge, 2005).
[10] S. H. Behrens and M. Borkovec, J. Chem. Phys. **111**, 382 (1999); M. Borkovec and S. H. Behrens, J. Phys. Chem. B **112**, 10795 (2008).
[11] M. Lund and B. Jönsson, Q. Rev. Biophys. **46**, 265 (2013).
[12] D. Chan, J. W. Perram, L. R. White, and T. W. Healy, J. Chem. Soc. Faraday Trans. 1 **71**, 1046 (1974); D. Chan, T. W. Healy, and L. R. White, *ibid.* **72**, 2844 (1976).
[13] R. Podgornik and V. A. Parsegian, Chem. Phys. **154**, 477 (1991).
[14] R. Podgornik and V. A. Parsegian, J. Phys. Chem. **99**, 9491 (1995).
[15] S. L. Carnie and D. Y. Chan, J. Colloid Interface Sci. **161**, 260 (1993).
[16] R. J. Nap, A. Lošdorfer Božič, I. Szleifer, and R. Podgornik, Biophys. J. **107**, 1970 (2014).
[17] N. Boon and R. van Roij, J. Chem. Phys. **134**, 054706 (2011).
[18] R. R. Netz, J. Phys.: Condens. Matter **15**, S239 (2003).
[19] M. Lund and B. Jönsson, Biochemistry **44**, 5722 (2005); F. L. B. da Silva, M. Lund, B. Jonsson, and T. Åkesson, J. Phys. Chem. B **110**, 4459 (2006); F. L. B. da Silva and B. Jonsson, Soft Matter **5**, 2862 (2009).
[20] B. W. Ninham and V. A. Parsegian, J. Theor. Biol. **31**, 405 (1971).
[21] N. Adžić and R. Podgornik, Eur. Phys. J. E **37**, 49 (2014).

[22] A. C. Maggs and R. Podgornik, Europhys. Lett. **108**, 68003 (2014).
[23] H. Li and M. Kardar, Phys. Rev. Lett. **67**, 3275 (1991).
[24] F. J. M. Ruiz-Cabello, P. Maroni, and M. Borkovec, J. Chem. Phys. **138**, 234705 (2013).
[25] G. Trefalt, F. J. Montes Ruiz-Cabello, and M. Borkovec, J. Phys. Chem. B **118**, 6346 (2014).
[26] M. Lund and B. Jönsson, Biophys. J. **85**, 2940 (2003).
[27] R. A. Curtis, J. Ulrich, A. Montaser, J. M. Prausnitz, and H. W. Blanch, Biotechnol. Bioeng. **79**, 4 (2002).